

Dynamical model calculation to reconcile the nuclear fission lifetime from different measurement techniques

M. T. Senthil Kannan,^{1,*} Jhiliam Sadhukhan,^{2,3,†} B. K. Agrawal,^{3,4} M. Balasubramaniam,¹ and Santanu Pal^{5,‡}

¹Department of Physics, Bharathiar University, Coimbatore-641046, India

²Physics Group, Variable Energy Cyclotron Center, Kolkata-700064, India

³Homi Bhabha National Institute, Mumbai-400094, India

⁴Saha Institute of Nuclear Physics, Kolkata-700064, India

⁵CS-6/1, Golf Green, Kolkata-700095, India



(Received 19 June 2018; published 2 August 2018)

The precission particle multiplicities suggest a lifetime of $\approx 10^{-20}$ s for nuclear fission to occur which is in contrast to the fission lifetime $\approx 10^{-18}$ s as predicted by an atomic probe. This long-standing ambiguity, arising due to the orders of magnitude differences among the fission lifetimes measured from the nuclear and atomic probes, has been addressed within a dynamical model which includes the contributions from the nuclear shell effects. We show that at lower excitation energies, these two probes decouple as the fissioning system survives for a long time without any particle evaporation. We also consider a wide range of reactions to study the impact of the excitation energy of the compound nucleus on the fission dynamics in general. Precission neutron multiplicity is found to be an inappropriate probe to measure fission lifetime at low excitation energy. In addition, our model predicts the average fission lifetime of the superheavy nucleus ³⁰²120 to be more than 10^{-18} s, which is in reasonable agreement with recent experiments.

DOI: [10.1103/PhysRevC.98.021601](https://doi.org/10.1103/PhysRevC.98.021601)

Introduction. Nuclear fission is a fundamental decay mode for very heavy atomic nuclei. The formation and survival of superheavy elements [1–4] is strongly governed by the associated reaction dynamics and, in particular, the fission probability. Moreover, the fission rate critically influences the origin of elements heavier than iron [5–7]. Therefore, a precise understanding of the fission lifetimes is of extreme importance.

Substantial effort has been made to measure fission lifetime. Traditionally, the precission charged-particle [8–12], neutron [9,11–20], and γ -ray [21–24] multiplicities are often used as a clock to estimate the fission time. The transient time also can be estimated by measuring the fission fragment distributions [25]. In general, all these nuclear techniques indicate that the fission process is fast enough with an upper bound in average fission time: $\langle \tau_f \rangle \leq 10^{-19}$ s. These nuclear probes encompass different variants of the dissipative model to bridge the experimental observables related to the fission lifetime. Often a simplified statistical model is assumed to mimic the actual dynamics [26,27]. On the other hand, the blocking technique in single crystals, which is considered to be a direct probe, leads to scission timescales much longer than the ones inferred from the nuclear methods [28,29]. This contradiction has intensified since several recent crystal-blocking measurements [30–33] have indicated attosecond (10^{-18} s) time delay in heavy-ion induced fission. It was shown recently that K x-ray emission

prior to fission can be used to measure fission lifetimes [34,35]. This method measures the long fission-time component in agreement with the crystal-blocking technique. Both atomic clocks are used to explore the survival of superheavy element with $Z = 120$ [32,35]. A detailed review of the study of fission lifetime can be found in Ref. [19].

Theoretical modeling of fission is extremely challenging as it involves many-body quantum dynamics. Recently, the self-consistent density functional theory was successfully applied to the studies of spontaneous fission and thermally induced fission. The spontaneous-fission half-lives are calculated using advanced energy density functionals [7,36,37]. Along this direction, the importance of nuclear pairing in spontaneous fission half-life has been demonstrated [38–40]. In the case of thermal fission, the time-dependent generator coordinator method assuming the Gaussian-overlap approximation was used successfully to study fission fragment distributions [41,42]. A thorough review of all these works is given in Ref. [43].

On the other hand, time-dependent density functional theory (TDDFT) methods have made substantial progress in describing low-energy thermal fission [44]. Recently, density fluctuations were incorporated within the TDDFT approach to generate spontaneous-fission yield distributions and kinetic energy distributions of fission fragments [45]. However, the situation becomes more complicated for induced fission from excited states, where pairing is quenched, a compound system is formed with a high angular momentum, and dynamics becomes strongly dissipative and nonadiabatic [46]. The use of a complete microscopic theory is prohibitively expensive to simulate the fission process of a rotating hot nucleus in

*senthilthulasiram@gmail.com

†jhiliam@vecc.gov.in

‡Formerly with Variable Energy Cyclotron Centre, Kolkata-700064, India.

coincidence with light particles and γ -ray evaporations. In this regime, stochastic transport theories have been successfully applied to describe the energy transfer between the collective and intrinsic degrees of freedom of the fissioning nucleus [26,47,48]. Among such theories, dynamical approaches based on the Langevin equation and its derivatives have been successful in reproducing fission dynamics [27,49–53].

In the present work, an explicit simulation of large-amplitude collective dynamics is performed, without incorporating any statistical model description, to extricate the long-standing ambiguities in fission lifetime measurements. Over the years, different theoretical propositions have been attempted to resolve the fission lifetime ambiguity [19,54,55]. Particularly, an unrealistically large dissipation strength has been used to reproduce the atomic-clock results [26,56]. The present work, for the first time, reproduces the atomic-clock data using the dissipation strength calculated from a realistic model. Moreover, the applicability of the nuclear probe is carefully scrutinized over a wide range of excitation energy.

Theoretical framework. We have implemented a state-of-the-art model based on the stochastic Langevin equation to study the full dynamical evolution of an excited compound system starting from the ground-state configuration up to scission. The Funny-Hills shape parameter c [57], which represents the elongation of a nucleus, is used as the collective coordinate. The one-dimensional Langevin equation [26,47,58] in terms of c is given as

$$\begin{aligned} \frac{dp}{dt} &= -\frac{p^2}{2} \frac{\partial}{\partial c} \left(\frac{1}{m(c)} \right) - \frac{\partial F}{\partial c} - \eta(c)p + g\Gamma(t), \\ \frac{dc}{dt} &= \frac{p}{m(c)}, \end{aligned} \quad (1)$$

where p is the momenta conjugate to c ; the strength of the random force g is related to the friction coefficient η through fluctuation-dissipation theorem: $g = \sqrt{\eta T}$ [47]. The shape-dependent collective inertia $m(c)$ is extracted using the Werner-Wheeler approximation [59,60] for the irrotational flow of incompressible nuclear fluid. The chaos-weighted wall friction model [60,61] is used to calculate the friction coefficient $\eta(c)$ as it seems to be most suitable for the present purpose [62–64]. The $\Gamma(t)$ represents the random force with the time correlation property $\langle \Gamma(t) \rangle = 0$ and $\langle \Gamma(t_1)\Gamma(t_2) \rangle = \delta(t_1 - t_2)$. The Helmholtz free energy F is used as the driving force for the collective motion. Specifically, we assumed the Fermi gas model [65] to define $F = V - (a - a_0)T^2$, where V and a are the deformation-dependent potential energy and level density parameter [66], respectively, a_0 being the value of a at the ground-state deformation. The energy- and deformation-dependent shell correction is incorporated in a following Ignatyuk's prescription [67]. The temperature T is obtained from the ground-state excitation energy E^* as $T = \sqrt{E^*/a_0}$. The average liquid-drop part of V is calculated following the double-folding Yukawa-plus-exponential model [48] and the associated shell-correction energy is obtained by applying Strutinsky's method [57,68] of shell correction to the nucleonic levels generated with the two-centered Woods-Saxon mean field [69]. We use the BCS pairing to account for nuclear superfluidity [57,69]. Calculated potential barriers are found to

be in good agreement with the existing results [70]. Langevin equations are solved numerically using the finite difference method [47]. For this purpose, we performed a second-order expansion of Eq. (1) in terms of small time increment δt . We consider $\delta t = 10^{-25}$ s in the present work. Large-scale computing is executed for an ensemble of 10^6 Langevin events to generate the results for a single macrostate. Each of the Langevin trajectories is allowed a maximum dynamical time of 10^{-15} s. For each event, the initial angular momentum of the compound nucleus is sampled from the corresponding fusion spin distribution. We consider the scission to occur when the neck radius of the compound nucleus becomes equal to $0.3R_0$ [57,59], R_0 being the spherical radius.

Evaporation of light particles n , p , α , and statistical γ rays are sampled at each time step of the dynamical evolution by using the Monte Carlo technique [26]. In case of any evaporation, the compound system and the associated energy and angular momentum are modified accordingly. Therefore, in advance, we calculate all the inputs for a total of 48 daughter nuclei, which leaves open the possibility of 15 neutron (n) evaporations in combination with either a proton (p) or an α evaporation. It ensures the scope of all the feasible evaporation channels for the present study. For each fission event, we record the average n -evaporation time τ_n , the time τ_{nl} when the last n is evaporated, and the scission time τ_f . According to the neutron clock [15], the product $\langle \tau_{n1} \rangle = n_{\text{pre}} \langle \tau_n \rangle$ gives the average fission lifetime, where n_{pre} is the average pre-scission neutron multiplicity. In practice, n -decay width, which is directly related to τ_n , is calculated and combined with a suitable fission-decay model to reproduce the experimental n_{pre} . Effectively, the measured n_{pre} determines the experimental fission lifetime [8,9,15]. Equivalently, the n clock can be devised using τ_{nl} with the underlying assumption that scission occurs immediately after the last neutron is evaporated. Of course, it may be violated in practice and the present work investigates the faith of this assumption *viz-a-viz* the applicability of the n clock. We compare these two neutron probes with the actual scission time τ_f . In addition, for a comprehensive understanding of the dynamical evolution, we calculate the average deformation $\langle d_f \rangle$ of the fissioning system by taking the time average of the collective coordinate for each event.

The present model avoids a major approximation of the existing combined dynamical and statistical model (CDSM) codes. In the case of CDSM [26,56,62,71,72], Langevin dynamics is performed up to an initial transient time (10^{-19} s in [26,56,62]) and then a suitable statistical model is used to decide the faith of the fission events. These statistical models usually consist of an approximate stationary fission width that neglects the details of deformation dependence of the input quantities. In contrast, dynamics is followed in the present work till the system bifurcates or an evaporation residue is formed. Further, the deformation-dependent shell effect is accounted for coherently within the potential energy and nuclear level density parameter.

Results and discussion. We first consider the $^{16}\text{O} + ^{208}\text{Pb} \rightarrow ^{224}\text{Th}$ reaction since this system is well studied experimentally [15,73]. The normalized yields corresponding to τ_n , τ_{nl} , and τ_f calculated for different values of initial excitation energy E^* are shown in Fig. 1. Evidently, at large

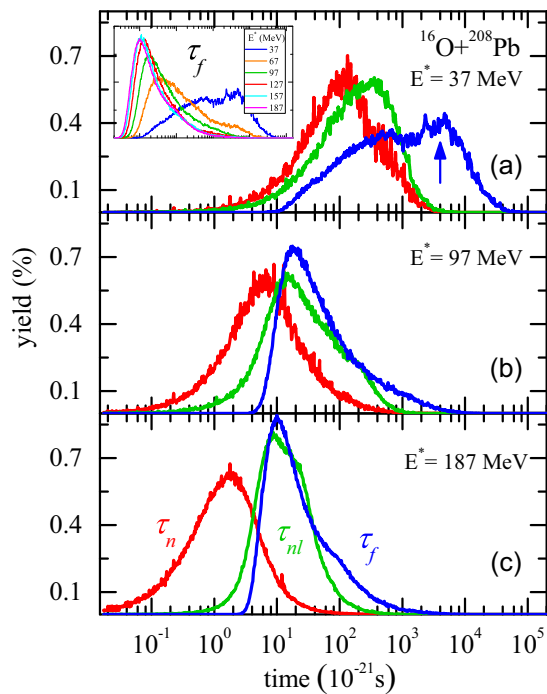


FIG. 1. Distributions of τ_f , τ_{nl} , and τ_n as labeled for initial excitation energy (a) $E^* = 37$ MeV, (b) $E^* = 97$ MeV, and (c) $E^* = 187$ MeV. Inset in (a) depicts the changeover of τ_f distributions with E^* . The peak of τ_f distribution for $E^* = 37$ MeV is indicated by an arrow.

E^* [Figs. 1(b) and 1(c)], the distributions of τ_{nl} and τ_f almost coincide except for the long-time tail in τ_f . This behavior of τ_f is reported in Refs. [26,71] using CDSM calculations. In contrast, for the lowest E^* [Fig. 1(a)], the shape of τ_f becomes very broad with the peak at $\tau_f > 10^{-18}$ s, whereas the shapes of τ_n and τ_{nl} remain almost unaffected. This decoupling of τ_f from τ_{nl} and τ_n appears somewhere between $E^* = 67$ and 37 MeV [inset of Fig. 1(a)]. It emphasizes the fact that at a lower energy, the fissioning system survives for a long time without any particle evaporation as the available excitation energy falls below the particle emission threshold. Additionally, we found that the long fission-time component is further enhanced by the nuclear shell effects as conjectured in [26,71].

For a deeper understanding of the nature of τ_f , we calculated the correlation between τ_f and $\langle d_f \rangle$. The corresponding two-dimensional distributions of fission events are plotted in Figs. 2(a) and 2(b), respectively, for the lowest and highest E^* considered in Fig. 1. Also, the free energy F for different values of T are shown in Fig. 2(c). Clearly, the events with a long fission time predominantly stay around the ground-state deformation ($0.95 \leq d_f \leq 1.1$). Here, $d_f = 1$ corresponds to the spherical configuration. On the other hand, the average deformation increases for the high-energy fission events as the free-energy profile becomes flatter. This observation clarifies the ambiguity related to the role of deformation-dependent dissipation in escalating fission lifetime. Since the majority of the long-time events roam around the ground-state deformation, these are hardly affected by dissipation near scission.

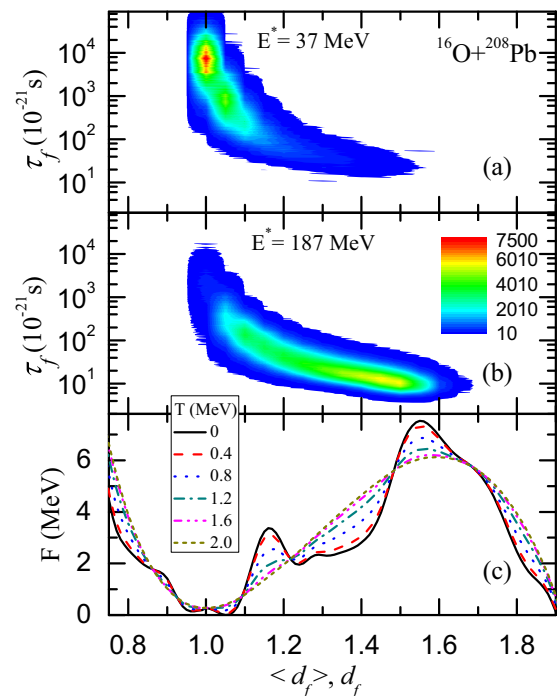


FIG. 2. Distribution of fission yields on the τ_f - $\langle d_f \rangle$ plane for (a) $E^* = 37$ MeV and (b) $E^* = 187$ MeV. (c) The variation of free energy F with deformation d_f for different temperatures as indicated.

We have calculated the average fission times $\langle \tau_f \rangle$, $\langle \tau_{nl} \rangle$, and $\langle \tau_n \rangle$ associated with the distributions of τ_f , τ_{nl} , and τ_n , respectively. These are plotted in Fig. 3(a) along with n_{pre} in Fig. 3(b). As expected, $\langle \tau_{nl} \rangle$ and $\langle \tau_n \rangle$ remain very close to each other at all energies. For higher E^* , $\langle \tau_f \rangle$ is comparatively large due to the presence of a long-time tail. Whereas, at low E^* , it is one order of magnitude higher than those for the other

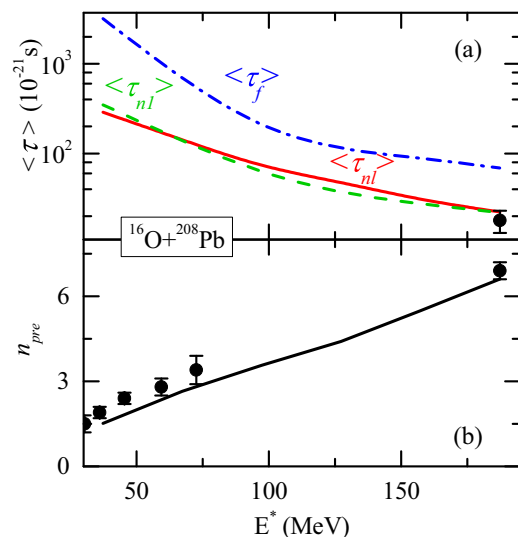


FIG. 3. (a) Average fission lifetime $\langle \tau_f \rangle$ (dash-dotted line), $\langle \tau_{nl} \rangle$ (dashed line), $\langle \tau_n \rangle$ (solid line) as a function of E^* . The symbol indicates the experimental data [15]. (b) Comparison of experimental [15,73] n_{pre} with the calculated values.

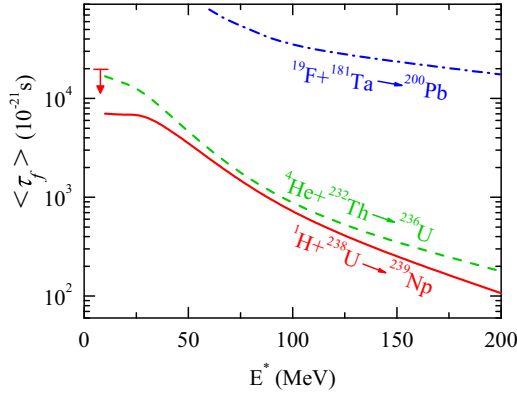


FIG. 4. Average fission lifetime ($\langle \tau_f \rangle$) as a function of excitation energy for the reactions (1)–(3) as mentioned in text.

two distributions due to the decoupling of τ_f from τ_{nl} and τ_n as shown in Fig. 1(a). Moreover, the absolute value of $\langle \tau_f \rangle$ reaches the attosecond timescale in agreement with atomic measurements. One experimental data of fission lifetime is available for the present system from neutron multiplicity measurement and it matches well with our calculated $\langle \tau_{nl} \rangle$ and $\langle \tau_{n1} \rangle$. It is clear from Fig. 3(b) that the experimental neutron multiplicities are reproduced simultaneously without any free parameter.

After the benchmark study on ^{224}Th , we computed the fission lifetime for several other reactions. Specifically, we considered the reactions (1) $p + ^{238}\text{U}$, (2) $^4\text{He} + ^{232}\text{Th}$, and (3) $^{19}\text{F} + ^{181}\text{Ta}$ covering a wide mass range relevant to fission. The excitation energy dependence of $\langle \tau_f \rangle$ for these reactions are demonstrated in Fig. 4. The $\langle \tau_f \rangle$ for both the actinides vary similarly and become slower than an attosecond for $E^* \leq 90$ MeV. This behavior is in compliance with the predictions from the atomic probe. The upper limit of $\langle \tau_f \rangle$ for reaction (1) is measured [28] for the lowest E^* (indicated by a down arrow in Fig. 4). As evident in Fig. 4, our calculation follows this limit. For reaction (3), $\langle \tau_f \rangle$ remains more than 10^{-17} s even at a very large E^* . This system has been studied extensively [74] around $E^* = 100$ MeV and, subsequently, analyzed theoretically in Ref. [56]. In their analysis, a comparatively large reduced friction was required within the dynamical model to delay fission. However, our calculation reproduces the lifetime of more than 10^{-17} s without recourse to the tuning of any input parameter. To determine the origin of the large fission lifetime, we extracted the distributions of τ_f , τ_{nl} , and τ_n (similar to Fig. 1) in Fig. 5. Interestingly, the second peak in τ_f has a substantial contribution between 10^{-17} and 10^{-15} s that results in a large $\langle \tau_f \rangle$. It appears because of a strong ground-state shell correction in ^{200}Pb that hinders the system from overcoming the barrier. Although this effect should disappear with excitation energy, the evaporation of neutrons helps it to persist even at high excitation energy. The presence of this broad second peak is consistent with the crystal-blocking data in Ref. [74].

Finally, we address the fission lifetime for the $^{238}\text{U} + ^{64}\text{Ni}$ reaction which is proposed to be a possible candidate for the discovery of $Z = 120$ isotopes. Several studies have been made

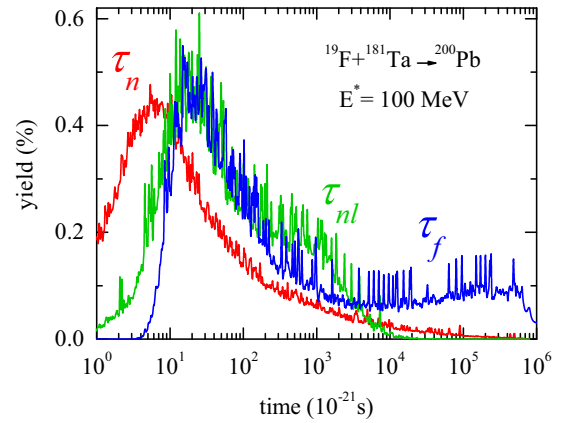


FIG. 5. Distributions of τ_f , τ_{nl} , and τ_n for the reaction $^{19}\text{F} + ^{181}\text{Ta}$.

to this end [32,35,54]. Crystal-blocking measurement [32] predicts that the $^{302}120$ nuclei can survive more than 10^{-18} s. In this experiment, the initial excitation energy of the compound system was uncertain due to the large target thickness. We found, as shown in Fig. 6, that $\langle \tau_f \rangle \geq 10^{-18}$ s is possible for this system only if the excitation energy $E^* \leq 10$ MeV (dashed lines). Therefore, the long-lived component in the experiment may be contributed from very low energy events. The stability of superheavy elements is very much sensitive to nuclear shell effects. Thus, an accurate estimation of nuclear potential energy surface is essential for a reliable prediction. In our calculation, the average fission barrier for $Z = 120$ isotopes is 9 MeV which is close to the microscopic density functional prediction [75]. The multidimensional macro-micro prediction [76] is 2 MeV smaller than this value. Although the fission lifetime is strongly influenced by the fission barrier, the temperature dependence of the potential surface apparently dilutes this effect. So, a proper modeling of the finite-temperature potential is crucial. Within the Fermi-gas model, the shell effect washes out much faster, as shown in Fig. 2(c), compared to the

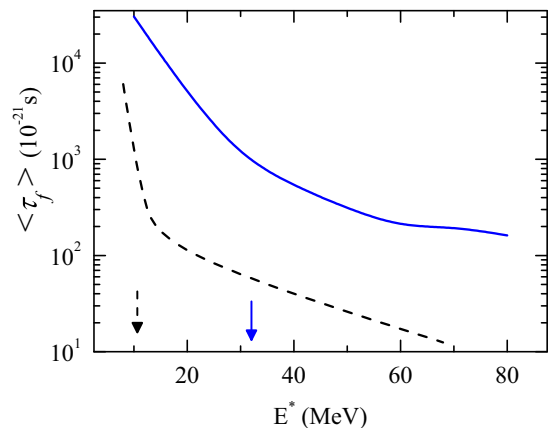


FIG. 6. Average fission lifetime as a function of excitation energy calculated with full (dashed line) and reduced (solid line) energy dependence in shell correction. Vertical arrows indicates the E^* corresponding to $\langle \tau_f \rangle = 10^{-18}$ s.

finite-temperature shell-model predictions [77]. To explore the effect of shell washing in the present system, we performed another set of calculations with a modified shell damping factor. Specifically, the energy dependence of the level density parameter a is reduced to 50% of its unaffected value.

The corresponding $\langle \tau_f \rangle$ is plotted in Fig. 6 and it shows that with this reduction, the attosecond time can be reached at a higher $E^* \approx 30$ MeV (solid line). This study reveals the importance of an appropriate microscopic calculation as far as superheavy elements are concerned.

Conclusions. A state-of-the-art calculation of fission dynamics is performed for excited compound systems where (i) the dynamics is followed from the ground-state deformation to scission including all possible evaporation channels, (ii) the energy- and deformation-dependent shell effect is properly accounted for, and (iii) no parameters are tuned to reproduce a specific observable. The discrepancy between the atomic and nuclear probes for the fission lifetime measurement is resolved by comparing the scission time with the indirect predictions

from evaporated neutrons. The neutron multiplicity probe is found to be inappropriate for estimating fission lifetime at low excitation energies. Our results comply with the crystal-blocking measurements for actinides. Also, we have shown that both measurement methods should agree at sufficiently high excitation energy where crystal-blocking data are still missing. Moreover, the attosecond fission timescale around the mass ≈ 200 region is reproduced with the same model parameters. Finally, for the generalization of our finding, calculation is performed for superheavy $Z = 120$ nucleus. The attosecond lifetime for $Z = 120$ nucleus is found to be consistent with our theoretical calculations.

Acknowledgments. Discussion with Nicolas Schunck is gratefully acknowledged. M.T.S. acknowledges the support and warm hospitality from CNT/VECC during his stay at VECC. Computing support for this work came from the Lawrence Livermore National Laboratory (LLNL) Institutional Computing Grand Challenge program and the computing facility at VECC.

-
- [1] S. Bjørnholm and J. E. Lynn, *Rev. Mod. Phys.* **52**, 725 (1980).
- [2] H. J. Krappe and K. Pomorski, *Theory of Nuclear Fission: A Textbook* (Springer, New York, 2012).
- [3] Y. T. Oganessian, V. K. Utyonkov, Y. V. Lobanov, F. S. Abdullin, A. N. Polyakov, I. V. Shirokovsky, Y. S. Tsyganov, G. G. Gulbekian, S. L. Bogomolov, B. N. Gikal, A. N. Mezentsev, S. Iliev, V. G. Subbotin, A. M. Sukhov, G. V. Buklanov, K. Subotic, M. G. Itkis, K. J. Moody, J. F. Wild, N. J. Stoyer, M. A. Stoyer, and R. W. Lougheed, *Phys. Rev. Lett.* **83**, 3154 (1999).
- [4] Y. T. Oganessian and V. K. Utyonkov, *Rep. Prog. Phys.* **78**, 036301 (2015).
- [5] G. Martínez-Pinedo, D. Mocolj, N. T. Zinner, A. Kelić, K. Langanke, I. Panov, B. Pfeiffer, T. Rauscher, K. H. Schmidt, and F. K. Thielemann, *Prog. Part. Nucl. Phys.* **59**, 199 (2007).
- [6] S. Goriely, J.-L. Sida, J.-F. Lemaître, S. Panebianco, N. Dubray, S. Hilaire, A. Bauswein, and H.-T. Janka, *Phys. Rev. Lett.* **111**, 242502 (2013).
- [7] S. A. Giuliani, G. Martínez-Pinedo, and L. M. Robledo, *Phys. Rev. C* **97**, 034323 (2018).
- [8] J. P. Lestone, J. R. Leigh, J. O. Newton, D. J. Hinde, J. X. Wei, J. X. Chen, S. Elfstrom, and D. G. Popescu, *Phys. Rev. Lett.* **67**, 1078 (1991).
- [9] J. P. Lestone, *Phys. Rev. Lett.* **70**, 2245 (1993).
- [10] J. Boger, J. M. Alexander, R. A. Lacey, and A. Narayanan, *Phys. Rev. C* **49**, 1587 (1994).
- [11] K. Ramachandran, A. Chatterjee, A. Navin, K. Mahata, A. Shrivastava, V. Tripathi, S. Kailas, V. Nanal, R. G. Pillay, A. Saxena, R. G. Thomas, S. Kumar, and P. K. Sahu, *Phys. Rev. C* **73**, 064609 (2006).
- [12] K. Kapoor, S. Verma, P. Sharma, R. Mahajan, N. Kaur, G. Kaur, B. R. Behera, K. P. Singh, A. Kumar, H. Singh, R. Dubey, N. Saneesh, A. Jhingan, P. Sugathan, G. Mohanto, B. K. Nayak, A. Saxena, H. P. Sharma, S. K. Chamoli, I. Mukul, and V. Singh, *Phys. Rev. C* **96**, 054605 (2017).
- [13] D. J. Hinde, R. J. Charity, G. S. Foote, J. R. Leigh, J. O. Newton, S. Ogaza, and A. Chatterjee, *Nucl. Phys. A* **452**, 550 (1986).
- [14] D. J. Hinde, D. Hilscher, and H. Rossner, *Nucl. Phys. A* **502**, 497 (1989).
- [15] D. J. Hinde, D. Hilscher, H. Rossner, B. Gebauer, M. Lehmann, and M. Wilpert, *Phys. Rev. C* **45**, 1229 (1992).
- [16] D. J. Hinde, *Nucl. Phys. A* **553**, 255 (1993).
- [17] K. Siwek-Wilczyński, J. Wilczyński, R. H. Siemssen, and H. W. Wilschut, *Nucl. Phys. A* **583**, 141 (1995).
- [18] J. Cabrera, T. Keutgen, Y. El Masri, C. Dufauquez, V. Roberfroid, I. Tilquin, J. Van Mol, R. Régimbart, R. J. Charity, J. B. Natowitz, K. Hagel, R. Wada, and D. J. Hinde, *Phys. Rev. C* **68**, 034613 (2003).
- [19] D. Jacquet and M. Morjean, *Prog. Part. Nucl. Phys.* **63**, 155 (2009).
- [20] S. Appannababu, M. Cinausero, T. Marchi, F. Gramegna, G. Prete, J. Bermudez, D. Fabris, G. Collazuol, A. Saxena, B. K. Nayak, S. Kailas, M. Bruno, L. Morelli, N. Gelli, S. Piantelli, G. Pasquali, S. Barlini, S. Valdré, E. Vardaci, L. Sajo-Bohus, M. Degerlier, A. Jhingan, B. R. Behera, and V. L. Kravchuk, *Phys. Rev. C* **94**, 044618 (2016).
- [21] M. Thoennessen, D. R. Chakrabarty, M. G. Herman, R. Butsch, and P. Paul, *Phys. Rev. Lett.* **59**, 2860 (1987).
- [22] P. Paul, *Nucl. Phys. A* **569**, 73 (1994).
- [23] G. van 't Hof, J. C. S. Bacelar, I. Diószegi, M. N. Harakeh, W. H. A. Hesselink, N. Kalantar-Nayestanaki, A. Kugler, H. van der Ploeg, A. J. M. Plompen, and J. P. S. van Schagen, *Nucl. Phys. A* **638**, 613 (1998).
- [24] D. J. Hofman, B. B. Back, I. Diószegi, C. P. Montoya, S. Schadmand, R. Varma, and P. Paul, *Phys. Rev. Lett.* **72**, 470 (1994).
- [25] C. Schmitt, P. N. Nadtochy, A. Heinz, B. Jurado, A. Kelić, and K.-H. Schmidt, *Phys. Rev. Lett.* **99**, 042701 (2007).
- [26] P. Fröbrich and I. I. Gontchar, *Phys. Rep.* **292**, 131 (1998).
- [27] K. Mazurek, P. N. Nadtochy, E. G. Ryabov, and G. D. Adeev, *Eur. Phys. J. A* **53**, 79 (2017).
- [28] F. Brown, D. A. Marsden, and R. D. Werner, *Phys. Rev. Lett.* **20**, 1449 (1968).
- [29] J. U. Andersen, E. Lægsgaard, K. O. Nielsen, W. M. Gibson, J. S. Forster, I. V. Mitchell, and D. Ward, *Phys. Rev. Lett.* **36**, 1539 (1976).

- [30] M. Morjean, M. Chevallier, C. Cohen, D. Dauvergne, J. Dural, J. Galin, F. Goldenbaum, D. Jacquet, R. Kirsch, E. Lienard, B. Lott, A. Peghaire, Y. Perier, J. C. Poizat, G. Prevot, J. Remillieux, D. Schmaus, and M. Toulemonde, *Nucl. Phys. A* **630**, 200 (1998).
- [31] J. U. Andersen, J. Chevallier, J. S. Forster, S. A. Karamian, C. R. Vane, J. R. Beene, A. Galindo-Uribarri, J. Gomez del Campo, H. F. Krause, E. Padilla-Rodal, D. Radford, C. Broude, F. Malaguti, and A. Uguzzoni, *Phys. Rev. Lett.* **99**, 162502 (2007).
- [32] M. Morjean, D. Jacquet, J. L. Charvet, A. L'Hoir, M. Laget, M. Parlog, A. Chbihi, M. Chevallier, C. Cohen, D. Dauvergne, R. Dayras, A. Drouart, C. Escano-Rodriguez, J. D. Frankland, R. Kirsch, P. Loutesse, L. Nalpas, C. Ray, C. Schmitt, C. Stodel, L. Tassan-Got, E. Testa, and C. Volant, *Phys. Rev. Lett.* **101**, 072701 (2008).
- [33] J. U. Andersen, J. Chevallier, J. S. Forster, S. A. Karamian, C. R. Vane, J. R. Beene, A. Galindo-Uribarri, J. G. del Campo, C. J. Gross, H. F. Krause, E. Padilla-Rodal, D. Radford, D. Shapira, C. Broude, F. Malaguti, and A. Uguzzoni, *Phys. Rev. C* **78**, 064609 (2008).
- [34] H. W. Wilschut and V. L. Kravchuk, *Nucl. Phys. A* **734**, 156 (2004).
- [35] M. O. Frégeau, D. Jacquet, M. Morjean, E. Bonnet, A. Chbihi, J. D. Frankland, M. F. Rivet, L. Tassan-Got, F. Dechery, A. Drouart, L. Nalpas, X. Ledoux, M. Parlog, C. Ciortea, D. Dumitriu, D. Fluerasu, M. Gugiù, F. Gramegna, V. L. Kravchuk, T. Marchi, D. Fabris, A. Corsi, and S. Barlini, *Phys. Rev. Lett.* **108**, 122701 (2012).
- [36] A. Staszczak, A. Baran, and W. Nazarewicz, *Phys. Rev. C* **87**, 024320 (2013).
- [37] J. Sadhukhan, K. Mazurek, A. Baran, J. Dobaczewski, W. Nazarewicz, and J. A. Sheikh, *Phys. Rev. C* **88**, 064314 (2013).
- [38] J. Sadhukhan, J. Dobaczewski, W. Nazarewicz, J. A. Sheikh, and A. Baran, *Phys. Rev. C* **90**, 061304 (2014).
- [39] S. A. Giuliani, L. M. Robledo, and R. Rodríguez-Guzmán, *Phys. Rev. C* **90**, 054311 (2014).
- [40] J. Zhao, B.-N. Lu, T. Nikšić, D. Vretenar, and S.-G. Zhou, *Phys. Rev. C* **93**, 044315 (2016).
- [41] H. Goutte, J. F. Berger, P. Casoli, and D. Gogny, *Phys. Rev. C* **71**, 024316 (2005).
- [42] D. Regnier, N. Dubray, N. Schunck, and M. Verrière, *Phys. Rev. C* **93**, 054611 (2016).
- [43] N. Schunck and L. M. Robledo, *Rep. Prog. Phys.* **79**, 116301 (2016).
- [44] A. Bulgac, P. Magierski, K. J. Roche, and I. Stetcu, *Phys. Rev. Lett.* **116**, 122504 (2016).
- [45] Y. Tanimura, D. Lacroix, and S. Ayik, *Phys. Rev. Lett.* **118**, 152501 (2017).
- [46] W. Nörenberg, *Nucl. Phys. A* **409**, 191 (1983).
- [47] Y. Abe, S. Ayik, P. G. Reinhard, and E. Suraud, *Phys. Rep.* **275**, 49 (1996).
- [48] A. J. Sierk, *Phys. Rev. C* **33**, 2039 (1986).
- [49] P. N. Nadtochy, E. G. Ryabov, A. E. Gegechkori, Y. A. Anischenko, and G. D. Adeev, *Phys. Rev. C* **85**, 064619 (2012).
- [50] Y. Aritomo, S. Chiba, and F. Ivanyuk, *Phys. Rev. C* **90**, 054609 (2014).
- [51] P. Möller and J. Randrup, *Phys. Rev. C* **91**, 044316 (2015).
- [52] V. Y. Denisov, T. O. Margitych, and I. Y. Sedykh, *Nucl. Phys. A* **958**, 101 (2017).
- [53] A. J. Sierk, *Phys. Rev. C* **96**, 034603 (2017).
- [54] A. K. Sikdar, A. Ray, and A. Chatterjee, *Phys. Rev. C* **93**, 041604 (2016).
- [55] A. Ray and A. K. Sikdar, *Phys. Rev. C* **94**, 055503 (2016).
- [56] Y. A. Lazarev, I. I. Gontchar, and N. D. Mavlitov, *Phys. Rev. Lett.* **70**, 1220 (1993).
- [57] M. Brack, J. Damgaard, A. S. Jensen, H. C. Pauli, V. M. Strutinsky, and C. Y. Wong, *Rev. Mod. Phys.* **44**, 320 (1972).
- [58] J. Sadhukhan and S. Pal, *Phys. Rev. C* **81**, 031602 (2010).
- [59] K. T. R. Davies, R. A. Managan, J. R. Nix, and A. J. Sierk, *Phys. Rev. C* **16**, 1890 (1977).
- [60] J. Sadhukhan and S. Pal, *Phys. Rev. C* **84**, 044610 (2011).
- [61] S. Pal and T. Mukhopadhyay, *Phys. Rev. C* **57**, 210 (1998).
- [62] T. Wada, Y. Abe, and N. Carjan, *Phys. Rev. Lett.* **70**, 3538 (1993).
- [63] G. Chaudhuri and S. Pal, *Phys. Rev. C* **65**, 054612 (2002).
- [64] G. Chaudhuri and S. Pal, *Phys. Rev. C* **63**, 064603 (2001).
- [65] A. Bohr and B. Mottelson, *Nuclear Structure* (Benjamin, New York, 1969), Vol. I.
- [66] W. Reisdorf, *Z Phys. A* **300**, 227 (1981).
- [67] A. V. Ignatyuk, M. G. Itkis, V. N. Okolovich, G. N. Smirenkin, and A. S. Tishin, *Yad. Fiz.* **21**, 1185 (1975) [*Sov. J. Nucl. Phys.* **21**, 612 (1975)].
- [68] V. M. Strutinsky, *Nucl. Phys. A* **122**, 1 (1968).
- [69] F. Garcia, O. Rodriguez, J. Mesa, J. D. T. Arruda-Neto, V. P. Likhachev, E. Garrote, R. Capote, and F. Guzmán, *Comput. Phys. Commun.* **120**, 57 (1999).
- [70] J. Dudek, W. Nazarewicz, and A. Faessler, *Nucl. Phys. A* **412**, 61 (1984).
- [71] I. I. Gontchar, M. Morjean, and S. Basnary, *Eur. Phys. Lett.* **57**, 355 (2002).
- [72] P. N. Nadtochy, G. D. Adeev, and A. V. Karpov, *Phys. Rev. C* **65**, 064615 (2002).
- [73] H. Rossner, D. J. Hinde, J. R. Leigh, J. P. Lestone, J. O. Newton, J. X. Wei, and S. Elfström, *Phys. Rev. C* **45**, 719 (1992).
- [74] J. Forster, I. Mitchell, J. Andersen, A. Jensen, E. Laegsgaard, W. Gibson, and K. Reichelt, *Nucl. Phys. A* **464**, 497 (1987).
- [75] A. Baran, M. Kowal, P. G. Reinhard, L. M. Robledo, A. Staszczak, and M. Warda, *Nucl. Phys. A* **944**, 442 (2015).
- [76] P. Möller, A. J. Sierk, T. Ichikawa, A. Iwamoto, R. Bengtsson, H. Uhrenholt, and S. Åberg, *Phys. Rev. C* **79**, 064304 (2009).
- [77] M. Brack and P. Quentin, *Phys. Lett. B* **52**, 159 (1974).